Organic & Biomolecular Chemistry

Cite this: *Org. Biomol. Chem.*, 2012, **10**, 7392

www.rsc.org/obc

PAPER

Resorcinarene-based cavitands with chiral amino acid substituents for chiral amine recognition†

Na Li, Fan Yang, Hillary A. Stock, David V. Dearden, John D. Lamb and Roger G. Harrison*

Received 23rd March 2012, Accepted 11th July 2012
DOI: 10.1039/c2ob25613d

Resorcinarene-based deep cavitands alanine methyl resorcinarene acid (**AMA**), alanine undecyl resorcinarene acid (**AUA**) and glycine undecyl resorcinarene acid (**GUA**), which contain chiral amino acids, have been synthesized. The upper rim of the resorcinarene host is elongated with four identical substituents topped with alanine and glycine groups. The structures of the new resorcinarenes were elucidated by nuclear magnetic resonance (NMR), mass spectrometry (MS) and the sustained *off*-resonance irradiation collision induced dissociation (SORI-CID) technique in FTICR-MS. These studies revealed that eight water molecules associate to the cavitand, two for each alanine group. The alanine substituent groups are proposed to form a kite-like structure around the resorcinarene scaffold. The binding of **AMA**, **AUA**, and **GUA** with chiral *R*- and *S*-methyl benzyl amines was studied by ^{1}H NMR titration, and compared to that of a binary L-tartaric acid and the monoacid phthalyl alanine (**PA**). The results show that these compounds interact with amine guests; however, with four carboxylic acid groups, they bind several amine molecules strongly while the binary L-tartaric acid only binds one amine guest strongly. The simple compound **PA**, which contains one carboxylic group, shows weak binding to the amines. The ^{1}H NMR titration of **AUA** with primary, secondary, and tertiary chiral amines showed that it can discriminate between these three types of amines and showed chiral discrimination for chiral secondary amines.

Introduction

Resorcinarenes are cyclic tetramers that are synthesized from the condensation of resorcinol and various aldehydes, as originated by Högberg[1] and further developed by Cram and co-workers.[2] These host molecules are relatively easy to synthesize in a wide range of sizes and functional groups.[3] They have applications in supramolecular recognition,[4] nanoscale reaction containment,[5] catalysis,[6] chiral NMR shift agents,[7] chromatographic separations,[8] and drug encapsulation, protection, and delivery.[9]

Chiral resorcinarene-based cavitands are rare, but have been prepared in several ways.[7b,10] One particularly effective approach is to introduce chiral substituent groups on the upper rim of the resorcinarene. It is hoped that the cavitand will bind guests having complementary functional groups by non-covalent interactions. In this way, the cavitand might selectively bind guests of proper size, shape, chirality, hydrophobicity, and surface charge characteristics. Usually, the binding of a guest is indicated by an upfield shift in the NMR signal of the guest due to shielding by the resorcinol rings.

Selective binding of enantiomers by macrocyclic ligands has significant potential application in separation of pharmaceuticals and enantioselective catalysis. Asymmetrically functionalized resorcinarenes were used as catalysts for the addition reaction of diethylzinc to benzaldehyde.[11] A bridged dimethoxy ketal diamine ligand containing asymmetric units was bonded to the upper rim of the resorcinarene and demonstrated enantioselectivity for (*R*)-1-phenyl propyl alcohol (ee 51%). Also, water-soluble resorcinarenes used as chiral NMR solvating agents for green chemistry applications and pharmaceutical delivery have been prepared.[7] Chiral NMR solvating agents associate with enantiomers selectively by non-covalent interaction and the resulting diastereomeric complexes may exhibit different chemical shifts in the NMR spectrum. As a result, chiral NMR solvating agents can be used to estimate the purity of enantiomers. The cavitands containing hydroxyproline groups demonstrated chiral discrimination for pyridyl, phenyl, and bicyclic aromatic substrates.

The synthesis of chiral resorcinarenes based on stereocenters atop elongated side panels to provide a deep pocket for substrate sequestration has been reported.[12] These hosts were shown to

Department of Chemistry and Biochemistry, Brigham Young University, Provo, UT 84602, USA. E-mail: roger_harrison@byu.edu; Fax: +1 801 422-0153; Tel: +1 801 422-8096

†Electronic supplementary information (ESI) available: NMR and MS of compounds, particle size analysis spectra. See DOI: 10.1039/c2ob25613d

discriminate between enantiomeric guests. The upper rim of a deepened resorcinarene was modified with Fmoc-protected chiral alanine chlorides to create a hydrophobic pocket with a chiral opening. Two sets of upfield NMR signals corresponding to the diastereomeric complexes formed by (+)- and (−)-pinanediol were observed. This work confirmed the feasibility of creating asymmetric deep resorcinarene-based cavitands by introducing chiral substituent groups on the upper rim. Amino acids have been used previously to modify such hosts, but in a very different configuration from that used in the work described herein.

In this paper, we report designed and characterized deep chiral cavitands using amino acid substituents on the upper rim of resorcinarenes. The elongated cavitand design has potential advantages. Specifically, different amino acids can be bonded to the resorcinarene and, as a result, the acidity of the host and design of the chiral center can be modified. The chiral alanine groups provide stereo centers, while the carboxylic acid groups concentrated on the upper rim can enhance the non-covalent interactions with guests *via* hydrogen bonding and electrostatic forces. Furthermore, the lower rim of the resorcinarenes can be modified with long alkyl chains making it possible to adsorb the compounds to a hydrophobic resin for separations applications.[8,13] We present a detailed structural study of the alanine containing resorcinarene and its binding to chiral primary, secondary and tertiary amines.

Results and discussion

The synthesis and characterization of these new amino acid containing cavitands provides host molecules with two major components, the resorcinarene scaffold and the quinoxaline panels. The resorcinarene scaffolds are formed in a one step process by combining alkyl aldehyde with resorcinol. Synthesis of the panels is a more complex process, and indeed it is through these that the amino acid functionality is introduced. To begin, 1,2-phenylenediamine is converted to the dichloropyrazine anhydride following published procedures (Scheme 1). The anhydride can be converted into the glycine or alanine-containing panel by addition of the amino acid ester. After this moiety is added to resorcinarene, the new cavitand is formed (**AME**, **AUE**, or **GUE**, Scheme 2). The undecyl chains are incorporated into some of the molecules to increase solubility in non-polar solvents. The cavitands have four pyrazine panels on the same face of the molecule, each with an amino acid group on its upper rim. To form the salts of the amino acids, sodium hydroxide is used to hydrolyze the ester. The salts can then be converted to the acids by addition of hydrochloric acid. The target molecule has four amino acid groups held in proximity to each other, bonded to heteroatoms containing five and six member rings. These will potentially be able to bind molecules through hydrogen bonding and dipole–dipole interactions.

NMR characterization

One of the well-known characteristics of resorcinarene-based cavitands is the conformational variation from C_{4v} to C_{2v}, namely from the vase structure to the kite structure. In the vase structure, the four substituent groups on the upper rim of the resorcinarene are positioned vertically, forming a large vase-shaped cavity; in the kite conformation, they are oriented outward, forming a flatter structure. The conformation is influenced by temperature and variations in pH. At low temperature, solvation energies stabilize the kite structure with its solvent-exposed surface; at high temperature, the entropic term predominates, and the vase structure is favored.[14] When the nitrogen atoms of the substituent groups on the resorcinarene are protonated under acidic conditions, the repulsion between protonated nitrogen atoms promotes the kite conformation.[15] The NMR chemical shift of the methine proton on the lower rim of resorcinarene (H_a) is usually found further downfield in the vase structure than in the kite structure, and this difference is symptomatic of compound conformation.

As mentioned above, the chemical shift of the methine proton H_a is usually considered an indicator of vase *versus* kite conformation. Specifically, in less polar solvents like chloroform, benzene, and THF, the methine proton of other compounds appears at $\delta \approx 5.5$ ppm or further downfield in the vase conformation and at $\delta \approx 3.7$ ppm in the kite conformation.[16] For our alanine-containing cavitand, **AME**, the chemical shifts of H_a in $CDCl_3$ and d_6-acetone are 4.069 and 4.077 ppm, respectively. These values are intermediate in chemical shift between cases of vase and kite structures reported,[16] but closer to kite conformation. Similar results were obtained for the glycine-containing analog **GUE**. Specifically, the chemical shifts of H_a in **GUE** in $CDCl_3$ and d_6-acetone are 4.145 and 3.925 ppm, respectively. These results imply that **AME** and **GUE** have relatively open kite-like structures in $CDCl_3$ and d_6-acetone.

^{1}H NMR experiments of **AME** in d_6-acetone and $CDCl_3$ at variable temperatures (VT-NMR) were performed to determine the conformation of the compound. The proton H_a on the

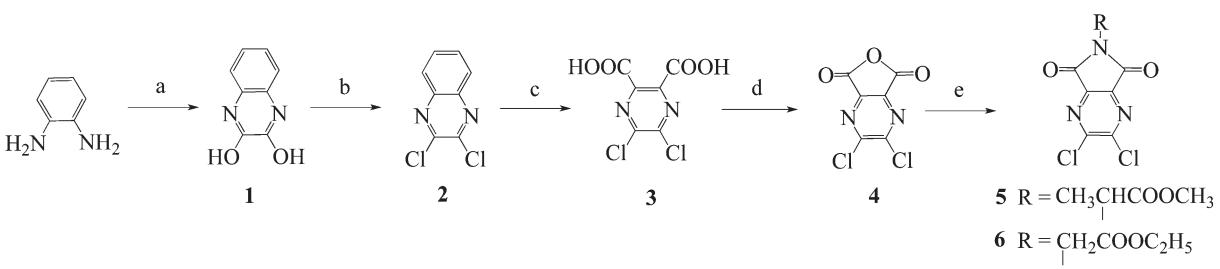

Scheme 1 Synthetic scheme for the amino acid containing pyrazine. Conditions: (a) oxalic acid, 2 M HCl, 2 h; (b) *N*,*N*-diethylaniline, phosphoryl chloride ($POCl_3$), 120 °C, 4 h; (c) $KMnO_4$, reflux, 1.5 h, HCl; (d) oxalyl chloride $(COCl)_2$, pyridine, dry THF, 0 °C 2 h, 50 °C 1 h; (e) L-alanine methyl ester hydrochloride or glycine ethyl ester hydrochloride in acetic anhydride, 120 °C, 2 h.

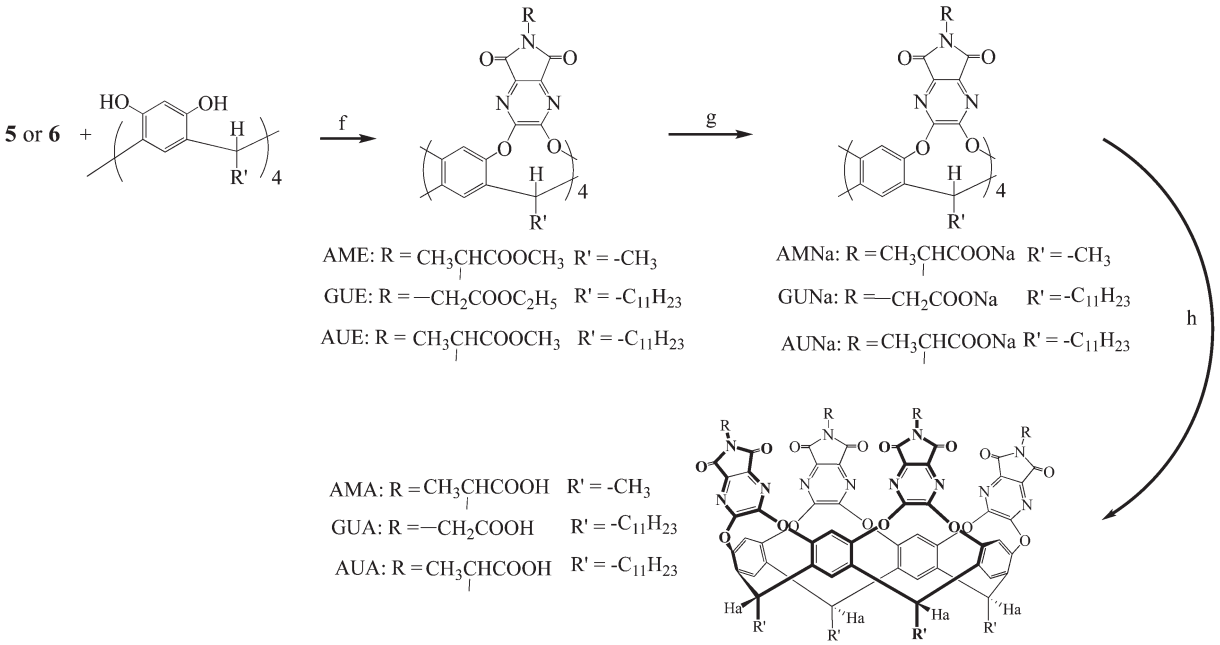

Scheme 2 Synthetic steps to form the amino acid containing resorcinarene cavitands. Conditions: (f) dry DMF, rt, 12 h; (g) THF, NaOH, 12 h; (h) HCl, H_2O.

methine group of the resorcinarene became broad, lost splitting and moved upfield (about 0.1 ppm), as temperature was lowered from 40 to −20 °C.† The signal of the two protons on the phenyl ring of the resorcinarene broadened and underwent coalescence as temperature was lowered. Others have reported that the phenyl protons of the resorcinarene divide into two singlets as the temperature is lowered, indicating conformation exchange between two kite structures.[15,16] However, we didn't find that the protons split into two singlets at lower temperature, implying that **AME** maintains a stable kite-like structure. Also, VT-NMR experiments were performed on **AMNa** and **AMA** to study their conformations in solution. The chemical shift of the methine proton H_a in **AMNa** (about 3.9 ppm) didn't change in D_2O from 9 to 60 °C. This implies that, like the ester analog, **AMNa** maintains a kite structure. Likewise, the chemical shifts of the acid analog **AMA** in d_6-DMSO didn't show any obvious movement from 23 to 80 °C, implying that **AMA** maintains a kite structure in DMSO.

After noting broad NMR signals for the acid and salt molecules, we realized they have polar and non-polar ends and might be aggregating. In polar solvents, the amino acid groups will be solvated while the alkyl chains might congregate to form micelle structures. Aggregate formation would result in protons not being able to freely rotate and thus chemically equivalent protons would be in different environments, making for broad NMR signals. The analysis using dynamic light scattering of the sodium salts (**AUNa**, **GUNa**, and **AMNa**) in water showed two major particle distributions, one at a small diameter particle size and another at a larger diameter.† The acids (**AUA**, **GUA**, and **AMA**) dissolved in methanol also showed two broad peaks for small and large diameter sized particles. This was different from what was seen for the esters (**AUE**, **GUE**, and **AME**), where only one small diameter particle peak was observed. Even when low concentrations of the salts and acids were analyzed, large diameter particles were observed. Thus, it looks like the salts and acids aggregate, which could explain their broad NMR signals.

Mass spectrometry characterization

To further characterize the new amino acid containing resorcinarenes, we used mass spectrometry. The mass spectrum of **AME** was obtained by dissolving it in mixed solvents of methanol and chloroform and operating in positive mode. We obtained a +1 molecular ion peak at *m*/*z* 1614.46. The mass difference between the calculated value and this experimental value (1469.25 amu) is 145.21 amu. A clue to the source of the difference was provided in the ^{1}H NMR spectrum of **AME**, which was sharp and clean and showed a water peak. We propose that this mass difference in the MS results from eight water molecules that are associated with **AME**. Thus, the calculated molecular peak for (**AME** + $8H_2O$) in positive mode is 1614.41 amu, which is consistent with the experimental value 1614.46 amu.

Along with characterizing the ester **AME** by mass spectrometry, we also used mass spectrometry to characterize the sodium salt and acid. First, the mass spectrum of **AMNa** in negative mode from methanol–water solvent was obtained (Fig. 1a). The largest peak observed was a minus two ion at 777.24 *m*/*z*. In order to better understand the spectrum of **AMNa**, we also prepared the analogous potassium and lithium salts, **AMK** and **AMLi**, and obtained their mass spectra for comparison (Fig. 1b and 1c). All compounds displayed a −2 peak around 777 *m*/*z* and several other higher mass peaks. For **AMNa**, the mass difference between the peak at 777 *m*/*z* and the next large peak at 788 *m*/*z* is 22 (when multiplied by 2 for charge considerations). Comparable differences were found for

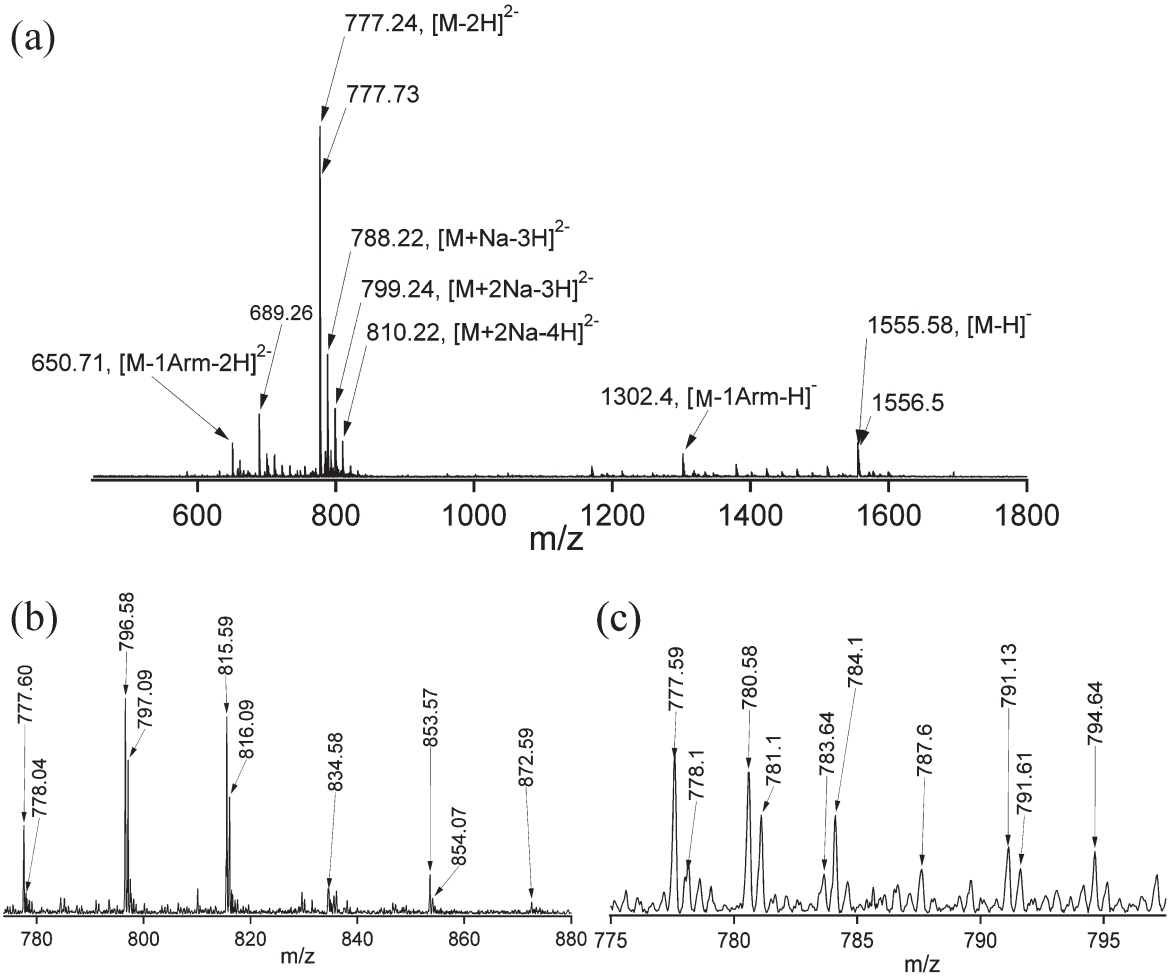

Fig. 1 The ESI mass spectra of (a) **AMNa**, (b) **AMK**, and (c) **AMLi** in negative ion mode.

AMK and **AMLi**. Specifically, these mass differences were about 38 and 6, respectively, which correspond to the addition of an alkali metal and loss of a proton. Based on these results, we concluded that in the negative MS mode, metal ions such as Li^+, Na^+, and K^+, can be dissociated from the cavitand molecule, leaving a stable −2 charged molecular ion (mass ≈ 777). This mass at 777 amu corresponds to a parent molecular ion of 1554 amu, which is 144 amu larger than the mass of **AMA**. This mass difference is the same mass as eight water molecules, implying that once again the cavitand associates with water in the MS. Although two THF molecules (144.12 amu), which was used as solvent during the synthesis of **AMNa**, have a similar mass to eight water molecules, it was not detected in the NMR and was not in the MS solvent. As with the ester, a water peak was observed in the NMR spectrum of **AMA**, however, its integration was less than eight water molecules per **AMA**. By elimination, we concluded that **AMNa** is associated with eight water molecules, just as was true for **AME**.

In order to shine further light on the structure of **AMNa** and its eight water molecules, SORI-CID FTICR MS was used to study it. SORI-CID MS is one of the more robust methods to study large ions and can provide complementary structural data to NMR. In SORI-CID, an *RF* pulse is applied slightly above or below the resonance frequency of the preselected ion, which causes the kinetic energy of the ion to increase, and allows the ion to collide repeatedly with background neutral gas molecules, such as N_2, Ar, or CO_2. As a result, the internal energy of the preselected ion increases, which causes fragmentation of the ion. Fragments of a chemical species, especially those that are not covalently bonded to the species, can be observed directly.

The ion with the highest intensity at 777.24 *m*/*z* was chosen and isolated from other fragments. An *RF* pulse was applied at slightly above the resonance frequency of this ion; nitrogen gas molecules were introduced to collide with this preselected ion and, as a result, the kinetic energy of the ion was converted to the internal energy necessary to fragment the ion. The resulting mass spectrum was recorded as shown in Fig. 2a. The −2 peaks at 755.2, 733.22, 711.22, and 689.23 *m*/*z* have a mass difference of 22, and this corresponds to the stepwise loss of CO_2 (mass 44), one from each carboxylic acid. The rate of the reduction of the 777 *m*/*z* peak corresponds to the increase in the other mass peaks (Fig. 2b). The loss of CO_2 is commonly found in SORI-CID for compounds containing carboxylic acid groups.[17] In addition, the mass difference between −2 peak 768.2 and 777.21 *m*/*z* is 9.1, which corresponds to the mass of a water molecule. Also, two water molecules were lost from peak 755.2 *m*/*z*,

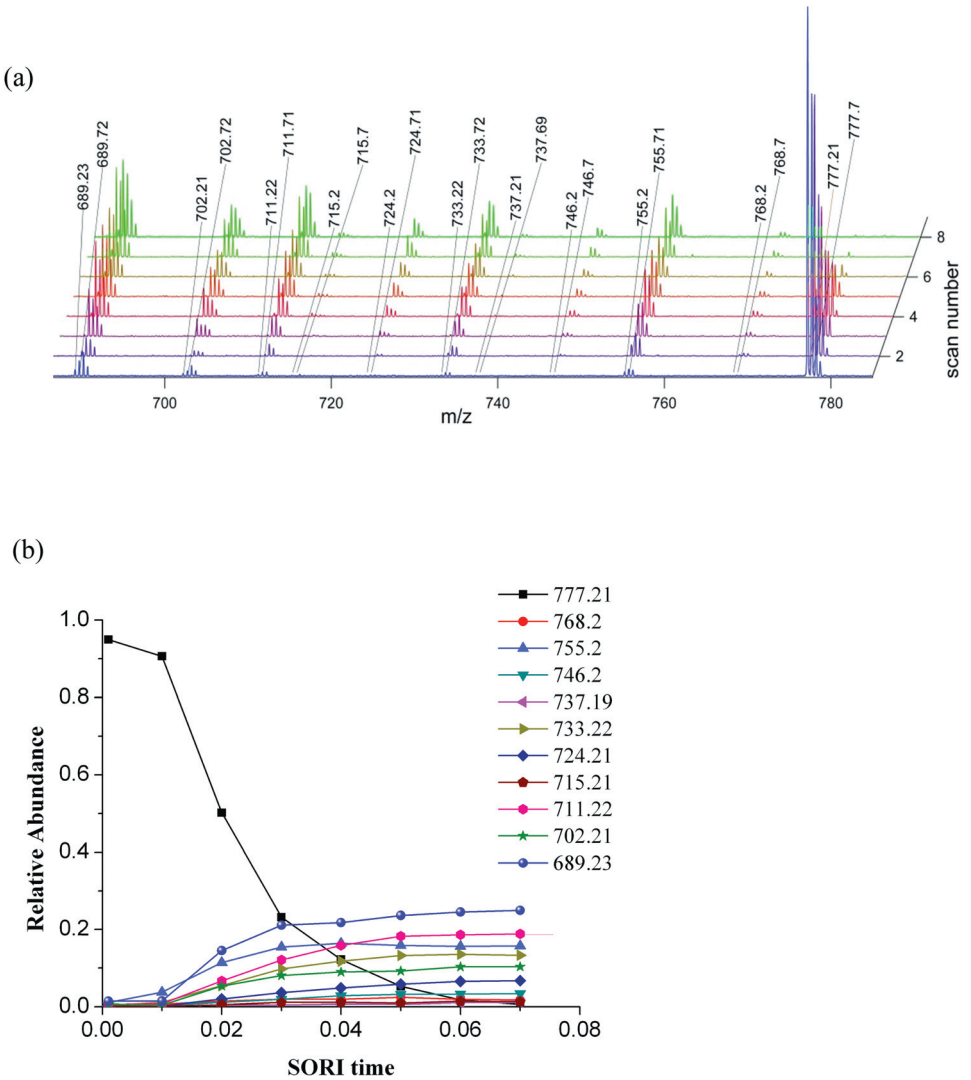

Fig. 2 Mass spectra analysis of **AMNa** by SORI-CID. (a) MS/MS spectrum of **AMNa** showing parent peak at 777 *m*/*z* and the fragments from it as they grow over time. (b) Relative abundance of fragment ions showing that as the quantity of the parent ion decreases, the quantity of the fragments increase.

with corresponding peaks at 746.2 and 737.19 *m*/*z*, respectively. The same situation was found after losing the second CO_2. The loss of the second CO_2 (peak at 733.22 *m*/*z*) was followed by the loss of two water molecules. The corresponding peaks appear at 724.21 and 715.21 *m*/*z*. These results indicate that two water molecules are associated with each carboxylic acid group. Once again, the results are consistent with the association between **AMNa** and eight water molecules. Thus, the −2 peak in the **AMNa** spectrum at 777.24 *m*/*z* corresponds to the addition of eight water molecules, loss of all sodium atoms and addition of two protons (calculated value: 777.17 *m*/*z*).

Mass spectrometry was also used to help characterize the acid **AMA**. The FTICR-MS spectrum of **AMA** in negative mode shows −1 and −2 molecular ion peaks at 1556.5 and 777.44 *m*/*z*, respectively (Fig. 3). The calculated molecular weight for **AMA** is 1413.14 amu and thus the mass difference between the experimental and calculated −1 molecular ion is 144 amu. Once again, we considered different possible guest molecules that might account for the mass difference. Specifically, we had added HCl to **AMNa** to prepare **AMA**. The molecules potentially associated with the cavitand would be HCl (mass of four HCl molecules = 143.92) or H_2O (mass of eight H_2O molecules = 144.08). We calculated the isotope distribution of **AMA** + 4HCl and **AMA** + $8H_2O$ and found the calculated isotope distribution of **AMA** + 4HCl is quite different from the experimental result in the size and distribution of peaks. The isotope distribution of **AMA** + $8H_2O$ is similar to what was found experimentally. Thus, we concluded that **AMA** is associated with eight water molecules.

We found an interesting regularity in the −1 MS spectrum of **AMA**. The mass difference between peaks 1556.5 and 1303.03 *m*/*z* is 253.47, which is almost exactly the mass of one amino acid substituent group and two OH groups. Furthermore, we found another peak at 1049.81 *m*/*z*, which corresponds to the loss of a second such group. We should note here that the two OH groups and the two protons left on the parent molecule are

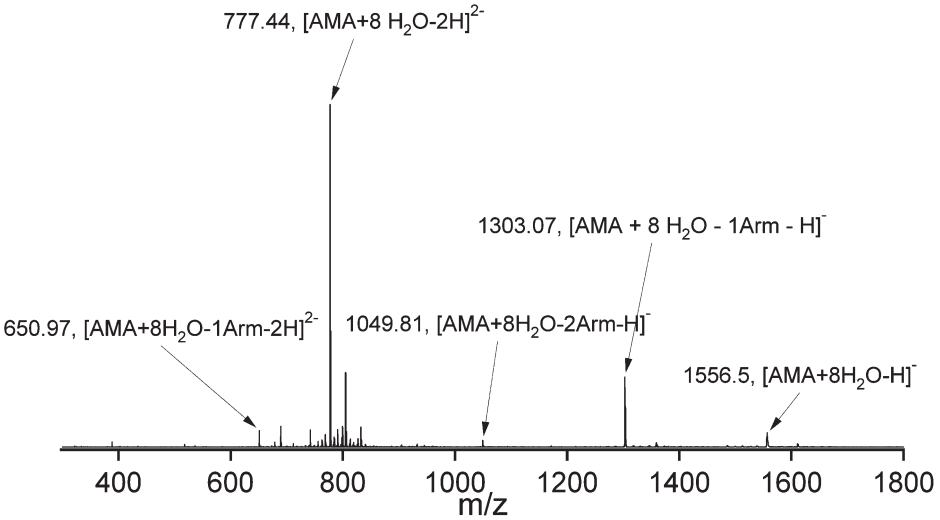

Fig. 3 Mass spectrum of **AMA** in negative mode (FTICR MS with ESI source).

most likely from water molecules. Based on these experimental results, we propose that each amino acid group is associated with two water molecules, which is consistent with the various MS experiments described above for **AMA** and **AMNa**.

MS studies of the glycine-containing **GUNa**, **GUA**, **AUNa**, and **AUA** yielded results similar to those with the alanine-containing cavitands described above. Specifically, molecular ion peaks belonging to **GUNa**·8H_2O, **GUA**·8H_2O, **AUNa**·8H_2O and **AUA**·8H_2O were obtained, which indicates that the designed substituent groups attached on the resorcinarene scaffold are quite hydrophilic and have great affinity to polar water molecules.

Amine discrimination

Since the alanine-containing cavitands carry chiral groups on the upper rim, experiments were conducted to examine the ability of these hosts to discriminate between enantiomeric guest molecules. The chiral discrimination of **AMA** and **AUA** between chiral amines was studied by ^{1}H NMR titration with the expectation that enantiomers may exhibit different chemical shifts upon complexation. The optical activity of **AMA** and **AUA** was studied by polarimetry, confirming that these molecules are chiral. Baseline NMR titration studies were performed using various compounds for comparison of results with **AMA**. These included ^{1}H NMR titration experiments associating *R*- and *S*-methyl benzyl amines (**1*R*** and **1*S***) with L-tartaric acid, phthalyl alanine (**PA**) (an analog of a cavitand side panel, Fig. 4), and **GUA**, a non-chiral analog of **AMA**. Also, NMR titration experiments of **AUA** with chiral secondary and tertiary amines (Fig. 4) were performed to further understand the interaction between **AUA** and amines.

When the chiral amines were titrated with **AMA**, **GUA**, tartaric acid and PA in DMSO, the chemical shift of the α-carbon proton moved downfield. The NMR titrations of the acids **AMA** and **GUA** with *R*- and *S*-methyl benzyl amines (**1*R*** and **1*S***), as well as the compounds chosen for baseline studies, are shown in Fig. 5. The observed chemical shift of the amine guest (δ_{Gobs}) can be expressed by the following equation: $\delta_{Gobs} = X_G\delta_G + X_{HG}\delta_{HG}$, where X_G is the fraction of free guest, δ_G is the chemical shift of free guest, X_{HG} is the fraction of host–guest complex, and δ_{HG} is the chemical shift of bound guest. When more amine is added into solutions of **AMA** and **GUA**, the guest protons are still shifted downfield, until over two equivalents of amine are added. Subsequently, the chemical shift slowly moves upfield to where it was without **AMA** or **GUA** present. For tartaric acid and **PA**, when amine is added to them, the amine chemical shifts return quickly to those of the free amine. The flat region of the titration curve reflects the binding capability of the host. **AMA** and **GUA** have four acid groups, tartaric acid has two and **PA** has one, thus **AMA** and **GUA** cause amine chemical shift changes over more equivalents of amine. The downfield shift of the amine protons may result from the neutralization reaction between the amine and the carboxylic acid groups on the host. When the **AMNa** salt is titrated with amine, the amine protons only slightly shift downfield and quickly return upfield with added amine.

The titration curves show that **AMA** and **GUA** bind methyl benzyl amines, but they do not show chiral discrimination. The curves for when the *R* and *S* isomers are added to **AMA** are similar to each other and indeed, they are similar to when the amines are added to the achiral **GUA** (Fig. 5). It is well known that if a guest is encapsulated in a cavitand, the ^{1}H NMR chemical shifts of the guest will appear more upfield due to the shielding of the guest by the cavity. However, we have not observed any upfield shift of guest protons.

Chiral secondary and tertiary amines were also titrated with **AUA** and the chemical shift change of the proton on the α-C of the amine was monitored. **AUA** showed distinct discrimination for primary, secondary, and tertiary amines (Fig. 6). The chemical shift changes most for the most basic amines – tertiary amines moved much more downfield (about 1.2 ppm) than less basic secondary and primary amines (0.8 and 0.45 ppm, respectively). As more amine was added, the chemical shift of the primary and secondary amines remained fairly constant for up to

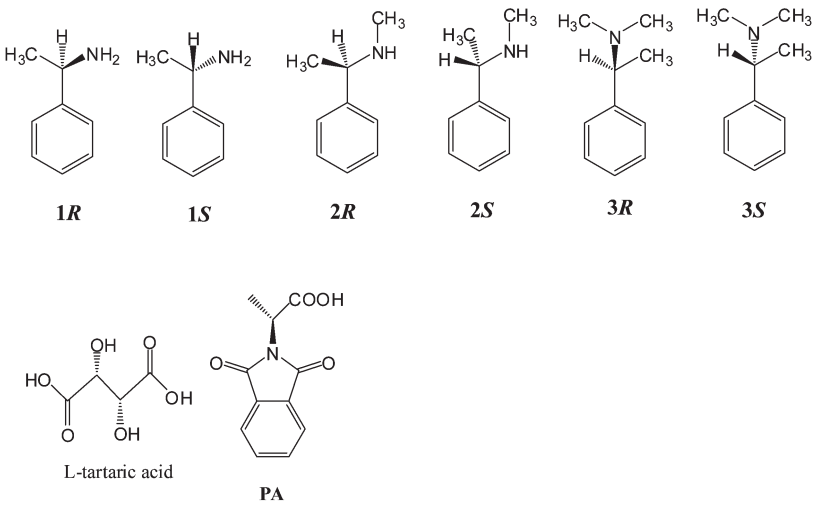

Fig. 4 Chiral benzyl amines used as guests for discrimination experiments (**1*R***, **1*S***, **2*R***, **2*S***, **3*R***, **3*S***) and chiral compounds (L-tartaric acid and **PA**) used as hosts.

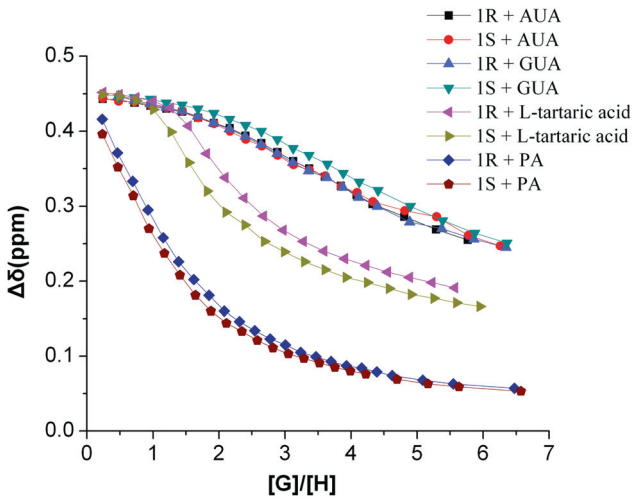

Fig. 5 ^{1}H NMR titrations of **AMA**, **GUA**, **PA**, and L-tartaric acid with *R*- and *S*-methyl benzyl amine (**1*R*** and **1*S***). The chemical shift change ($\Delta\delta$) of the proton on the α-C of the amine is plotted *versus* the ratio of amine to host molecule ([G]/[H]).

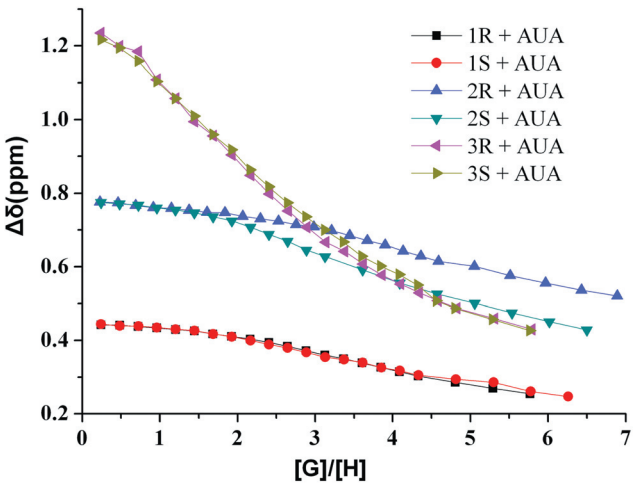

Fig. 6 ^{1}H NMR titrations of **AUA** with chiral primary (**1*R*** and **1*S***), secondary (**2*R*** and **2*S***), and tertiary amines (**3*R*** and **3*S***). The chemical shift change ($\Delta\delta$) of the proton on the α-C of the amine is plotted *versus* the ratio of amine to **AUA** ([G]/[H]).

two equivalents of amine and then began to go back upfield. This indicates that for primary and secondary amines, the first amine equivalents interact strongly with **AUA**. However, the chemical shift of the tertiary amine moved back upfield when more amine was added, which indicates that the equilibrium between the protonated and non-protonated tertiary amines shifts to the non-protonated form more easily than it does for the other amines. The titration curves of the enantiomeric primary amines are almost overlapped, as are those of the chiral tertiary amines, which indicates that there is no chiral discrimination of **AUA** for primary and tertiary amines. However, chiral discrimination of **AUA** for chiral secondary amines was observed after about 2 equivalents of amine were added.[18] These titration experiments were repeated and the results were consistent. The chiral discrimination occurs in the region of weaker guest binding.

Conclusions

The structure characterization of chiral cavitands **AMA**, **AUA**, **GUA** indicated that they have four amino acid groups on their upper rim. The electrospray mass spectroscopic characterization showed eight water molecules associated to the cavitands. The comparison of NMR titration curves of **AMA**, **GUA**, L-tartaric acid, and **PA** with *R*- and *S*-methyl benzyl amines showed that **AMA** and **GUA** bind more amine guests strongly than monoacid **PA** and binary acid L-tartaric acid. The ^{1}H NMR titration experiments with chiral primary, secondary, and tertiary amines showed that **AUA** causes different chemical shift changes for these three types of amines. Also, **AUA** shows chiral discrimination for secondary amines at greater than two equivalents.

Experimental

General methods

Deuterated NMR solvents were obtained from Cambridge Isotope Laboratories, Inc. All other chemical reagents were used as supplied from Aldrich Chemical Inc., unless otherwise noted. The resorcinarenes were synthesized using the method of Högberg,[1] employing acetaldehyde to yield the methyl-substituted version and undecyl aldehyde for the undecyl-substituted version. Compounds **1**,[19] **2**,[20] **3**,[21] and **4**,[21] as well as phthalyl alanine (**PA**),[22] were synthesized according to published methods. For clarity, in this paper we refer to individual resorcinarene compounds using acronyms constructed as follows: **A** or **G** = alanine or glycine substitution on the resorcinarene upper rim; **M** or **U** = methyl or undecyl substitution on the resorcinarene lower rim; **E**, **A**, or **Na** = ester, acid, or sodium salt of the amino acid.

^{1}H and ^{13}C NMR spectra were recorded using a VXR 500-MHz multinuclear FT-NMR spectrometer. Proton (^{1}H) chemical shifts (δ) were reported in parts per million with respect to tetramethylsilane (TMS, δ = 0 ppm) or solvent peaks. Most of the mass spectrometric experiments were performed on a Bruker model APEX 47e Fourier transform ion cyclotron resonance (FTICR) mass spectrometer with a MIDAS system.[23] The microelectrospray ionization (ESI) source with a heated metal capillary drying tube was modified based on the design of Eyler.[24] The typical operating flow rate of the ESI source was 10 μL h^{-1}. Compounds **5**, **6** and **AME** were acquired in positive mode on an Agilent 1100 LC/MS series with ESI source. The Zetasizer nano ZS dynamic light scattering instrument (Malvern instrument, Malvern, Worcestershire, UK) was used to analyze the particle size distribution of the compounds. Melting points were determined using a SRS DigiMelt MPA 160 apparatus from Stanford Research Systems, Inc. Optical rotations were measured using a Perkin-Elmer 241 polarimeter (sodium D-line, 529 nm) and $[\alpha]_D^{23}$ values are given in 10^{-1} deg cm^2 g^{-1}, concentration (c) in g per 100 mL. Elemental analyses were performed by M-H-W Laboratories, Phoenix, AZ.

Methyl 2-(2,3-dichloro-5,7-dioxo-5*H*-pyrrolo[3,4-*b*]pyrazin-6-(7*H*)-yl) propanoate (5). 5,6-Dichloropyrazine-2,3-dicarboxylic acid anhydride (**4**, 0.4380 g, 2 mmol) and L-alanine methyl ester hydrochloride (0.5030 g, 3.6 mmol) were put in a closed container. 2 mL of acetic anhydride were added to the mixture and it was stirred at 120 °C for 2 h and then was poured into 20 mL of distilled water. The yellow precipitate that formed was filtered and dried under vacuum for 2 h (0.400 g, 65.8% yield). Mp: 119–120 °C. ^{1}H NMR (500 MHz, d$_6$-acetone): δ (ppm) = 1.658 (d, J = 28, 3H), 3.726 (s, 3H), 5.146 (q, J = 28, 1H). ^{13}C NMR (500 MHz, d$_6$-acetone) δ (ppm): 170.2, 162.8, 153.5, 145.3, 53.3, 48.9, 15.3. $[\alpha]_D^{23}$ = −32.0 (c 1.00, acetone). MS (MH$^+$, ESI) m/z 305.16 (calculated: 305.09).

Ethyl 2-(2,3-dichloro-5,7-dioxo-5*H*-pyrrolo[3,4-*b*]pyrazin-6-(7*H*)-yl) acetate (6). 5,6-Dichloropyrazine-2,3-dicarboxylic acid anhydride (**4**, 0.4380 g, 2 mmol) and glycine ethyl ester hydrochloride (0.5025 g, 3.6 mmol) were put in a closed container. 2 mL of acetic anhydride were added to the mixture and it was stirred at 120 °C for 2 h and then was added to 20 mL of distilled water. The yellow precipitate was filtered and dried under vacuum for 2 h (0.450 g, 74.0% yield). Mp: 133–134 °C. ^{1}H NMR (500 MHz, d$_6$-acetone) δ (ppm): 1.265 (t, J = 30, 3H), 4.208 (q, J = 28, 2H), 4.561 (s, 2H). ^{13}C NMR (500 MHz, d$_6$-acetone) δ (ppm): 167.6, 162.8, 153.7, 145.3, 62.6, 40.1, 14.4. MS (MH$^+$, ESI) m/z 305.18 (calculated: 305.09).

Alanine methyl resorcinarene ester (AME). Compound **5** (0.1000 g, 0.329 mmol) and methyl-resorcinarene (0.0404 g, 0.075 mmol) with methyl groups on the lower rim were put in a 10 mL two-necked flask connected to a condenser and a nitrogen gas inlet. 2.5 mL of dry dimethyl formamide (DMF) were added to the flask. Triethylamine (TEA) (0.0756 g, 0.75 mmol) was mixed with 0.50 mL of dry DMF and injected into the flask drop-wise. The mixture was stirred at room temperature for 12 h and the white precipitate that formed was filtered under vacuum. The filtrate was evaporated by rotary evaporator and the white solid was purified by column chromatography with eluent ethyl acetate and hexane (v : v 3 : 1) to yield 0.0583 g (53.1%). ^{1}H NMR (500 MHz, CDCl$_3$) δ (ppm): 1.705 (d, J = 18, 12H), 1.714 (d, J = 12, 12H), 3.726 (s, 12H), 4.069(q, J = 28, 4H) 5.012 (q, J = 28, 4H), 6.915(s, 4H), 7.345 (s, 4H). ^{1}H NMR (500 MHz, d$_6$-acetone) δ (ppm): 1.505 (d, J = 30, 12H), 1.585 (d, J = 28, 12H), 3.566 (s, 12H), 4.077 (q, J = 28, 4H), 4.932 (q, J = 30, 4H), 7.156 (s, 8H). ^{13}C NMR (500 MHz, d$_6$-acetone) δ (ppm): 170.4, 163.4, 152.5, 141.6, 135.2, 53.1, 48.4, 32.8, 17.8, 15.5. $[\alpha]_D^{23}$ = −16.2 ± 0.0 (c 1.00, acetone). MS [(M + 8H$_2$O + H)$^+$, ESI] m/z 1614.46 (calculated: 1614.37).

Alanine methyl resorcinarene sodium salt (AMNa). Compound **AME** (0.1000 g) was dissolved in 3 mL of tetrahydrofuran (THF) and 0.100 g of NaOH in 10 mL of H$_2$O were added. The mixture was refluxed for 12 h until the water layer became clear. The solvent was evaporated and the solid was washed with CH$_2$Cl$_2$ and extracted with H$_2$O. The H$_2$O layer was collected and evaporated. A red solid was obtained and the yield was 0.0780 g (76.3%). ^{1}H NMR (500 MHz, D$_2$O,) δ (ppm): 1.240 (br, 12 H), 1.407 (d, J = 30, 12H), 4.121 (br, 4H), 4.288 (q, J = 28, 4H). ^{13}C NMR (500 MHz, D$_2$O) δ (ppm): 180.2, 173.4, 171.0, 161.3, 51.2, 50.9, 50.6, 48.8, 17.5, 17.4. $[\alpha]_D^{23}$ = 34.6 ± 0.8 (c 1.00, H$_2$O). FTICR-MS [(M + 8H$_2$O − 4Na + 2H)$^{2-}$, ESI)] m/z 777.24 (calculated: 777.17). The Li and K salts were synthesized in a similar manner except that LiOH and KOH were used instead of NaOH.

Alanine methyl resorcinarene acid (AMA). Compound **AMNa**, 0.1 g, was dissolved in H$_2$O and acidified with diluted HCl (2 M). The yellow precipitate that formed was filtered, dissolved in methanol and filtered. The filtrate was evaporated by rotary evaporator to yield 0.0842 g (89.4%) of the title compound. ^{1}H NMR (500 MHz, d$_6$-DMSO) δ (ppm): 1.260 (br, 12 H), 1.409 (br, 12H), 3.925 (br, 4H), 4.291 (br, 4H). ^{13}C NMR (500 MHz, D$_2$O) δ (ppm): 173.4, 155.7, 148.5, 48.6, 42.0, 17.5. $[\alpha]_D^{23}$ = +11.2 ± 0.4 (c 1.00, methanol). FTICR-MS [(M + 8H$_2$O − H)$^-$, ESI)] m/z 1556.50 (calculated: 1556.28).

Glycine undecyl resorcinarene ethyl ester (GUE). Compound **6** (0.1 g, 0.329 mmol) and undecyl-resorcinarene (0.0825 g, 0.075 mmol) were put in a 10 mL two-necked flask connected to a condenser and nitrogen gas inlet. 2.5 mL of dry DMF were

added to the flask. TEA (0.0756 g, 0.75 mmol) was mixed with 0.5 mL of dry DMF and injected into the flask drop-wise. The mixture was stirred at room temperature for 12 h. The large amount of white precipitate that formed was removed by filtration. The filtrate was evaporated to dryness by rotary evaporator and the white solid purified by column chromatography with ethyl acetate and hexane as eluents ($v:v$ 3 : 1), yielding 0.1207 g of the title compound (79.6%). ^{1}H NMR (500 MHz, $CDCl_3$,) δ (ppm): 0.88 (t, J = 28, 12H), 1.25 (b, 72H), 1.39 (t, J = 32, 12H), 4.14 (s, 4H), 4.19 (q, J = 30, 8H), 4.48 (s, 8H), 6.93 (s, 4H), 7.45 (s, 4H). ^{1}H NMR (500 MHz, d_6-acetone) δ (ppm): 0.75 (t, J = 30, 12H), 1.12 (b, 84H), 2.10 (s, 12H), 3.92 (t, J = 30, 4H), 4.07 (q, J = 28, 8H), 4.36 (s, 8H), 7.10 (s, 4H), 7.20 (s, 4H). ^{13}C NMR (500 MHz, d_6-acetone) δ (ppm): 168.0, 163.7, 153.1, 142.1, 134.5, 126.2, 62.5, 39.8, 38.4, 32.8, 23.5, 32.0, 28.0, 14.5. Anal. calcd for $C_{112}H_{132}N_{12}O_{24}{\cdot}8H_2O$: C 61.86, H 6.86, N 7.73%; found: C 61.98, H 7.03, N 7.99%. MS [$(M + 8H_2O + H)^+$, ESI] m/z 2174.97 (calculated: 2174.04).

Glycine undecyl resorcinarene sodium salt (GUNa). GUE (0.1 g) was dissolved in 3 mL of THF and 0.1 g of NaOH in 10 mL of H_2O were added. The mixture was refluxed for 12 h until the water layer became clear. The solvent was evaporated and the solid was washed with CH_2Cl_2 and extracted with H_2O. The H_2O layer was collected, evaporated and yielded 0.0878 g (88.0%) of a red solid. ^{1}H NMR (500 MHz, D_2O) δ (ppm): 0.84 (br, 12 H), 1.24 (br, 72H), 1.82 (br, 8H), 3.56 (br, 4H), 3.91 (br, 8H). ^{13}C NMR of GUNa (500 MHz, D_2O) δ (ppm): 177.1, 165.7, 119.1, 43.6, 43.2, 31.9, 29.7, 22.6, 13.9. FTICR-MS GUNa [$(M + 8H_2O - 4Na)^{4-}$, ESI)] m/z 514.27 (calculated: 514.22).

Glycine undecyl resorcinarene acid (GUA). Compound **GUNa**, 0.1 g, was dissolved in H_2O and acidified with diluted HCl (2 M). The yellow precipitate that formed was filtered, dissolved in methanol and filtered. The filtrate was evaporated to dryness by rotary evaporator and yielded 0.0880 g of the title compound (92.0%). ^{1}H NMR (500 MHz, d_6-DMSO) δ (ppm): 0.82 (t, J = 24, 12 H), 1.21 (br, 72H), 1.78 (br, 8H), 3.76 (br, 8H), 3.92 (br, 4H). ^{13}C NMR (500 MHz, d_6-acetone) δ (ppm): 42.5, 33.0, 23.6, 14.7. Anal. calcd for $C_{104}H_{116}N_{12}O_{24}{\cdot}8H_2O$: C 60.57, H 6.45, N 8.15%; found: C 60.73, H 6.64, N 7.98%. FTICR-MS [$(M + 8H_2O - 2H)^{2-}$, ESI)] m/z 1030.10 (calculated: 1030.11).

Alanine undecyl resorcinarene methyl ester (AUE). Compound **5** (0.1 g, 0.329 mmol) and undecyl-resorcinarene (0.0825 g, 0.075 mmol) were put in a 10 mL two-necked flask connected to a condenser and nitrogen gas inlet. 2.5 mL of dry dimethyl formamide (DMF) were added to the flask. Triethylamine (TEA) (0.0756 g, 0.75 mmol) was mixed with 0.5 mL of dry DMF and injected into the flask drop-wise. The mixture was stirred at room temperature for 12 h and the white precipitate that formed was removed. The filtrate was evaporated by rotary evaporator and the white solid was purified by column chromatography with eluent ethyl acetate and hexane ($v:v$ 3 : 1) to yield 0.1359 g of the title compound (89.7%). ^{1}H NMR (500 MHz, $CDCl_3$) δ (ppm): 0.879 (t, J = 28, 12H), 1.25 (s, 72H), 1.69 (d, J = 28, 12H), 2.100 (d, J = 24, 8H), 3.713 (s, 12H), 4.196 (t, J = 28, 4H) 5.011 (q, J = 30, 4H), 6.929 (s, 4H), 7.457 (s, 4H). ^{1}H NMR (500 MHz, d_6-acetone) δ (ppm): 0.88 (t, J = 28, 12H), 1.27 (m, 72H), 1.64 (d, J = 30, 12H), 2.21 (d, J = 20, 8H), 3.68 (s, 12H), 4.04 (t, J = 32, 4H), 5.06 (q, J = 30, 4H), 7.22 (s, 4H), 7.32 (s, 4H). ^{13}C NMR (500 MHz, d_6-acetone) δ (ppm): 170.5, 163.5, 153.0, 141.8, 134.5, 126.1, 53.1, 48.4, 32.4, 23.4, 15.5, 14.5. $[\alpha]_D^{23}$ = −2.57 ± 0.0 (c 1.00, $CHCl_3$). Anal. calcd for $C_{112}H_{132}N_{12}O_{24}{\cdot}H_2O$: C 65.67, H 6.59, N 8.21%; found: C 65.72, H 6.64, N 8.03%. MS [$(M + 8H_2O + H)^+$, ESI] m/z 2174.94 (calculated: 2175.04).

Alanine methyl resorcinarene sodium salt (AUNa). AUE (0.1 g) was dissolved in 3 mL of tetrahydrofuran (THF) and 0.1 g of NaOH in 10 mL of H_2O were added. The mixture was refluxed for 12 h until the water layer became clear. The solvent was evaporated and the solid was washed with CH_2Cl_2 and extracted with H_2O. The H_2O layer was collected and evaporated to dryness to yield 0.0780 g (76.3%) of a red solid. ^{1}H NMR (500 MHz, D_2O,) δ (ppm): 0.78 (br, 12 H), 1.17 (br, 84 H), 1.85 (d, 8H), 3.99 (br, 4H), 4.23 (br, 4H). ^{13}C NMR (500 MHz, D_2O) δ (ppm): 180.2, 173.4, 171.0, 161.3, 51.2, 50.9, 50.6, 48.8, 17.5, 17.4. FTICR-MS [$(M + 8H_2O - 2Na - H)^{3-}$, ESI)] m/z 719.67 (calculated: 719.77).

Alanine undecyl resorcinarene acid (AUA). Compound **AUNa**, 0.1 g, was dissolved in H_2O and acidified with diluted HCl (2 M). The yellow precipitate that formed was filtered, dissolved in methanol and filtered. The filtrate was evaporated by rotary evaporator to yield 0.0862 g of the title compound (90.0%). ^{1}H NMR (500 MHz, d_6-DMSO) δ (ppm): 1.26 (br, 12 H), 1.41 (br, 12H), 3.92 (br, 4H), 4.29 (br, 4H). ^{13}C NMR (500 MHz, d_6-acetone) δ (ppm): 42.5, 33.0, 23.6, 14.7. $[\alpha]_D^{23}$ = 4.48 ± 0.4 (c 1.00, methanol). Anal. calcd for $C_{108}H_{124}N_{12}O_{24}{\cdot}8H_2O$: C 61.23, H 6.66, N 7.93%; found: C 61.31, H 6.75, N 7.78%. FTICR-MS AUA [$(M + 8H_2O - 3H)^{3-}$, ESI)] m/z 744.99 (calculated: 705.11).

NMR and ^{1}H NMR titrations. All of the ^{1}H NMR titration experiments were performed in d_6-DMSO. The samples (5 mM, 500 μL) **AMA**, **GUA**, L-tartaric acid, and **PA** were placed in individual NMR tubes. Microliter aliquots of amine guests **1*R***, **1*S***, **2*R***, **2*S***, **3*R***, and **3*S*** (100 mM) in d_6-DMSO were added drop-wise to the solutions. The chemical shift changes of the amine guests were monitored after each addition. The titration curves were obtained by plotting the $\Delta\delta$ of the methyl group of the amine against the concentration ratio of the sample to the amine.

Mass spectrometry. The FTICR-MS sustained off-resonance irradiation collision-induced dissociation (SORI-CID)[23] method was used to elucidate the structure of the resorcinarene and its complexes. In these experiments, the target peak of interest was isolated using stored waveform inverse Fourier transform (SWIFT) techniques, and the off-resonance excitation was applied for 5 s at 1 kHz below the resonance frequency of the ion of interest. The collision gas, high purity nitrogen, was pulsed into the ICR cell by a Freiser-type pulsed leak valve[25] and a 10 s delay was used to allow the background pressure in the trapping cell to drop from 10^{-5} mbar to the baseline pressure (about 10^{-8} mbar) prior to detection.

Dynamic light scattering. The instrument was operated at 25 °C with a detection angle of 90°. The esters (**AME** 1.1 mM,

AUE 0.68 mM, and **GUE** 0.65 mM) were dissolved in chloroform and filtered through filter paper (2.7 μm pore size, Whatman, USA). The sodium salts (**AMNa** 0.81 mM, **AUNa** 0.63 mM, and **GUNa** 0.64 mM) and the acids (**AMA** 0.92 mM, **AUA** 0.64 mM, and **GUA** 0.75 mM) were dissolved in distilled water and methanol, respectively, and filtered with a 25 mm syringe filter with a 0.45 μm polyethersulfone membrane (VWR international, USA).

Acknowledgements

The authors express appreciation to Dionex Corporation for graduate student support for NL and to Brigham Young University for financial support as well as for professorship funding to JDL.

Notes and references

1 A. G. S. Högberg, *J. Org. Chem.*, 1980, **45**, 4498.
2 J. R. Moran, S. Karbach and D. J. Cram, *J. Am. Chem. Soc.*, 1982, **104**, 5826.
3 (*a*) C. Wieser, C. B. Dieleman and D. Matt, *Coord. Chem. Rev.*, 1997, **165**, 93; (*b*) B. Purse and J. Rebek Jr., *Proc. Natl. Acad. Sci. U. S. A.*, 2005, **102**, 10777.
4 A. Szumna, *Chem. Commun.*, 2009, 4191.
5 P. Restorp and J. Rebek Jr., *J. Am. Chem. Soc.*, 2008, **130**, 11850.
6 R. J. Hooley and J. Rebek Jr., *Org. Biomol. Chem.*, 2007, **5**, 3631.
7 (*a*) R. Yanagihara, M. Tominaga and Y. Aoyama, *J. Org. Chem.*, 1994, **59**, 6865; (*b*) N. H. Pham and T. J. Wenzel, *J. Org. Chem.*, 2011, **76**, 786; (*c*) C. M. O'Farrell, J. M. Chudomel, J. M. Collins, C. F. Dignam and T. J. Wenzel, *J. Org. Chem.*, 2008, **73**, 2843; (*d*) C. M. O'Farrell, K. A. Hagan and T. J. Wenzel, *Chirality*, 2009, **21**, 911.
8 J. Wang, R. G. Harrison and J. D. Lamb, *J. Chromatogr. Sci.*, 2009, **47**, 510.
9 W. Śliwa and C. Kozlowski, *Calixarenes and Resorcinarenes: Synthesis, Properties and Applications*, Wiley-VCH, Verlag GmbH & Co. KGaA, Weinheim, Germany, 2009.
10 (*a*) B. Botta, F. Caporuscio, D. Subissati, A. Tafi, M. Botta, A. Filippi and M. Speranza, *Angew. Chem., Int. Ed.*, 2006, **45**, 2717; (*b*) B. Kuberski, M. Pecul and A. Szumna, *Eur. J. Org. Chem.*, 2008, **18**, 3069; (*c*) M. J. Mclldowie, M. Mocerino and M. I. Ogden, *Supramol. Chem.*, 2010, **22**, 13; (*d*) W. Iwanek and A. Wzorek, *Mini-Rev. Org. Chem.*, 2009, **6**, 398; (*e*) A. Szumna, *Chem.–Eur. J.*, 2009, **15**, 12381.
11 G. Arnott, H. Heaney, R. Hunter and P. C. B. Page, *Eur. J. Org. Chem.*, 2004, **24**, 5126.
12 (*a*) S. Saito, C. Nuckolls and J. Rebek Jr., *J. Am. Chem. Soc.*, 2000, **122**, 9628; (*b*) E. Mann and J. Rebek Jr., *Tetrahedron*, 2008, **64**, 8484.
13 B. R. Edwards, A. P. Giauque and J. D. Lamb, *J. Chromatogr., A*, 1995, **706**, 69.
14 J. R. Moran, J. L. Ericson, E. Dalcanale, J. A. Bryant, C. B. Knobler and D. J. Cram, *J. Am. Chem. Soc.*, 1991, **113**, 5707.
15 L. D. Shirtcliff, H. Xu and F. Diederich, *Eur. J. Org. Chem.*, 2010, **5**, 846.
16 (*a*) V. A. Azov, A. Beeby, M. Cacciarini, A. G. Gheetham, F. Diederich, M. Frei, J. K. Gimzewski, V. Gramlich, B. Hecht, B. Jaun, T. Latychevskaia, A. Lieb, Y. Lill, F. Marotti, A. Schlegel, R. R. Schlittler, P. J. Skinner, P. Seiler and Y. Yamakoshi, *Adv. Funct. Mater.*, 2006, **16**, 147; (*b*) D. J. Cram, H. J. Choi, J. A. Bryant and C. B. Knobler, *J. Am. Chem. Soc.*, 1992, **114**, 7748.
17 (*a*) B. Kanawati and P. Schmitt-Kopplin, *Rapid Commun. Mass Spectrom.*, 2010, **24**, 1198; (*b*) L. J. Cui, M. A. Isbell, Y. Chawengsub, J. R. Falck, W. B. Campbell and K. Nithipatikon, *J. Am. Soc. Mass Spectrom.*, 2008, **19**, 569.
18 Equilibrium constants were calculated using the titration data after the chemical shifts began to return to their original values.† The equilibrium constants are relative to each other. The calculated constants (log *Ks*) for the amines are: **1*R*** = 0.95; **1*S*** = 0.97; **2*R*** = 1.36; **2*S*** = 0.84; **3*R*** = 0.31, **3*S*** = 0.35. As is predicted from a qualitative view of Fig. 6, the tertiary amines bind the weakest and the secondary *R* isomer binds slightly more strongly than the secondary *S* isomer.
19 D. R. Romer, *J. Heterocycl. Chem.*, 2009, **46**, 317.
20 C. V. R. Sastry, M. Jogibhukta, V. S. H. Krishnan, P. S. Rao, K. Vemana, D. R. Shridhar, R. M. Tripathi, R. K. Verma and R. Kaushal, *Indian J. Chem. B Org.*, 1988, **27**, 1110.
21 V. A. Azov, P. J. Skinner, Y. Yamakoshi, P. Seiler, V. Gramlich and F. Diederich, *Helv. Chim. Acta*, 2003, **86**, 3648.
22 J. H. Billman and W. F. Harting, *J. Am. Chem. Soc.*, 1948, **70**, 1473.
23 H. Z. Zhang, E. S. Paulsen, K. A. Walker, K. E. Krakowiak and D. V. Dearden, *J. Am. Chem. Soc.*, 2003, **125**, 9284.
24 J. Laskin and J. H. Futrell, *Mass Spectrom. Rev.*, 2005, **24**, 135.
25 C. Q. Jiao, D. R. A. Ranatunga, W. E. Vaughn and B. S. Freiser, *J. Am. Soc. Mass Spectrom.*, 1996, **7**, 118.